INTERNATIONAL JOURNAL OF INTEGRATED ENGINEERING
ISSN: 2229-838X e-ISSN: 2600-7916

IJIE

Vol. 16 No. 5 (2024) 214-223
https://publisher.uthm.edu.my/ojs/index.php/ijie

Patient-Specific Design of Prosthesis for Below Knee Amputee: Analysis Between Different Gait

Muhammad Hanif Baharuddin[1], Amir Mustakim Ab Rashid[1], Nik Nur Ain Azrin Abdullah[1], Muhammad Hanif Ramlee[1,2]*

[1] *Bone Biomechanics Laboratory (BBL), Department of Biomedical Engineering and Health Science, Faculty of Electrical Engineering, Universiti Teknologi Malaysia, Johor Bahru, 81310, MALAYSIA*
[2] *Bioinspired Devices and Tissue Engineering (BIOINSPIRA) Research Group, Universiti Teknologi Malaysia, Johor Bahru, 81310, MALAYSIA*

*Corresponding Author: muhammad.hanif.ramlee@biomedical.utm.my
DOI: https://doi.org/10.30880/ijie.2024.16.05.017

Article Info

Received: 16 November 2023
Accepted: 11 June 2024
Available online: 1 August 2024

Keywords

Amputee, cost, design, prosthetic leg

Abstract

Major that often associated with prosthetic leg are poor comfort and high cost. The study is conducted to construct custom-made passive below knee prosthesis and to analyse the response to applied load in different gait condition. The scope of the study is the utilization of three-dimensional printing material, acrylonitrile butadiene styrene (ABS) in the manufacturing of prosthetic leg socket and pylon whereas the foot made from polyurethane. By using the Sense three-dimensional scanner, the subject's residual leg was scanned. SolidWorks and Meshmixer were the software used for the three-dimensional designing of prosthetic leg parts. By using 3-Matic, aligning and meshing were carried out. von Mises stress and displacement of model applied with axial load were obtained from simulation using Marc Mentat. The load applied for midstance, heel strike and toe off phases were 350 N, 1545 N and 2450 N, respectively. The constraints position was different for each phase. The peak stress of the model was reported during toe off (20.86 MPa) followed by heel strike (13.41 MPa) and midstance (4.89 MPa). The stress during all three phases not exceeding the yield of respective materials. In displacement, the model experience highest displacement (54.95 MPa) during toe off and the lowest during midstance (6 mm). In conclusion prosthetic leg with ABS components shows acceptable durability during different gait.

1. Introduction

Amputation of a limb is a physical impairment that affects physical structures and restricts everyday activities. Diabetes Mellitus (DM), trauma, and peripheral vascular disease are several causes of lower limb amputation. In Malaysia, DM is the most reported cause of amputation, accounted for 63 % of all cases of amputation [1]. For lower limb amputation, transtibial amputation being the most prevalent amputation type [1]. When compared to non-amputees, amputees move slower and have less stability. Amputee frequently utilize a lower-limb prosthetic to reinstate their aesthetic and impaired functions [2]. The prosthesis creates a composite biomechanical system whose behaviour is impacted by a number of circumstances when used by amputee [3]. The impact of different prosthetic components on individual with lower extremity amputation walking has been researched. For instance, prosthetic socket that not fit well to stump and failure suspension system can cause pistoning, that affects the gait patterns [4]. The only definite restrictions to particular prescriptions for a patient who is an applicant for a prosthesis are size and expense. Almost all parts are made in adult sizes, but children's

selections are significantly more restricted. Besides, expensive components may be prohibited by medicare restrictions or other insurance reimbursement regulations.

To re-establish as much normal gait as feasible is the fundamental objective of lower limb amputee rehabilitation. The proper mechanisms should be utilized in prosthetic devices to permit normal gait function [4]. To properly assess the gait characteristics of patients who have had lower limb amputations, the clinician must be familiar with both normal gait and the 'typical gait abnormalities' that are commonly seen in those who have had limbs amputated [5]. Gait anomalies in below-knee amputees include higher energy consumption, slower walking speeds and asymmetries between unilateral amputees' legs in the stance phase cycle, maximum vertical force, and step length [6]. Skin damage and pain may be experienced by amputee if the load inappropriately distributed on the residual limb during gait. In lower-limb prostheses, FEA is the most commonly used numerical analytical approach. During crucial stages of the gait cycle, the stress experienced by soft tissues over the residual leg were generally measured [3]. FEA has the potential to provide understanding into soft tissue load magnitudes and distributions, thus providing a verification foundation to aid prosthetists in designing socket, permitting rehabilitation to be hastened with treatment cost and less discomfort [7]. The failure of prosthetic leg components can also be predicted via FEA by comparing the peak stress to the elastic limit of material.

While the need for effective prosthetic legs is growing, the technology is still too expensive for many individuals. a number of developers have created prosthetic devices at a lower cost fabrication method to solve the problem such as implementing three-dimensional printing. From previous research, Rohjoni et al., developed a low-cost active prosthetic leg by utilizing 3D printer for prosthetic leg parts such as foot, pylon and ankle. The strength of the parts was evaluated via finite element analysis (FEA). They found out that the model FEA findings can be improved by increasing the pylon diameter [8]. Research conducted by Rochlitz and Pamer where their goal was to create a new low-cost energy store and return (ESAR) foot with innovative design and fabrication technologies. The tensile strength and modulus of the Acrylonitrile Butadiene Styrene (ABS) were utilized in simulation in terms of mechanical characteristics. Each of the three support stages of the walking cycle (powered plantar flexion/push-off, controlled dorsiflexion and controlled plantar flexion phase) was evaluated in the FEA [9].

The purpose of this study is to construct a low budget and patient specific design prosthetic leg to cater the problems in cost and design of prosthetic leg. Prosthesis components design was constructed by using SolidWorks and Autodesk Meshmixer. The end design was simulated in Marc Mentat to analyse the von Mises stress and displacement. Simulation results gave the insight on the potential of low-cost, three-dimensional printing materials which is Acrylonitrile butadiene styrene (ABS) to be implemented in prosthetic leg parts fabrication. The end design of prosthetic leg is simulated in three different gait phases which are during midstance, toe off and heel strike with varied magnitude of load applied and position of constraints region respectively.

2. Material and Methods

Before final results were obtained, several steps involving three-dimensional scanning, designing, meshing, aligning and analysis were performed.

2.1 Materials Three-Dimensional Scanning of Patient's Stump

An amputee aged 50 years old who fulfilled the required criteria such as transtibial amputee, experience prosthetic leg user who able to walk independently and possessed good pulmonary condition was recruited. His weight and height were 70kg and 167 cm respectively. Before his involvement in the whole study, the patient was given the consent form as proof for voluntarily participating in the scanning process and given approval for his residual leg 3D model to be used for designing and simulation (ethical approval no: UTMREC-2023-25). Before the 3D scanning procedure initiated, the subject was placed at a position where the scanner operator can access 360 degrees around the residual leg. The right residual leg of the patient was three-dimensional (3D) scanned as shown in Fig. 1 utilizing the handheld and portable, optical Sense 3D scanner (Sense 3D, 3D Systems, Inc., USA). The 3D scanner was moved with slowly and steady motion surrounding the stump of the subject to prevent the sensor from loss tracking of the residual leg structure [10]. The distance between the scanner and the residual leg was adjusted accordingly to ensure that the residual leg can be detected by the scanner. The scanned leg was modified using 3-Matic (Materialise N.V., Belgium) software as shown in Fig. 2 to eliminate unnecessary parts and noise before proceeding to prosthetic socket designing.

Int. Journal of Integrated Engineering Vol. 16 No. 5 (2024) p. 214-223

Fig. 1 *Three-dimensional scanning of patient's residual leg*

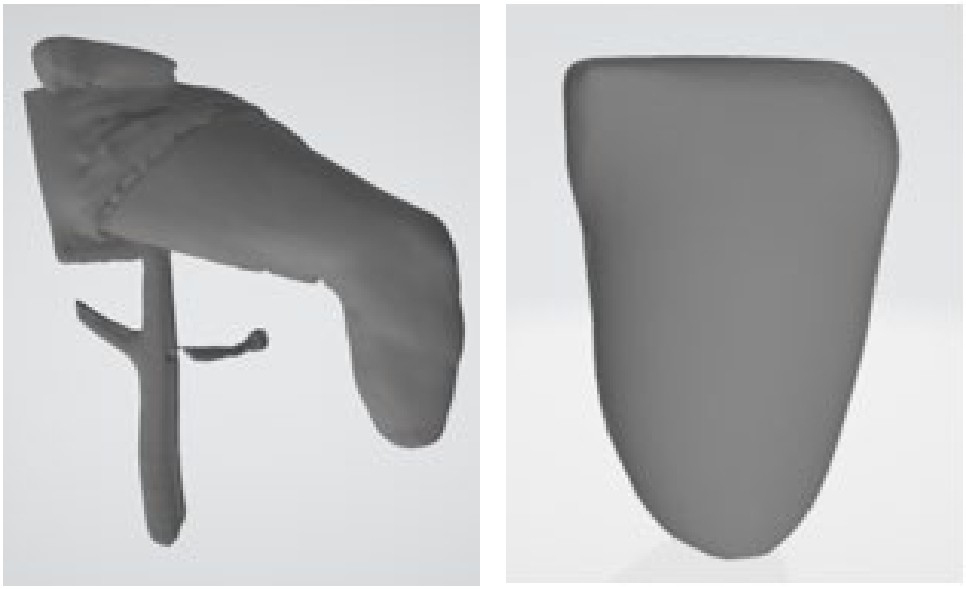

(a) **(b)**

Fig. 2 *3D model (a) pre-processed; (b) post-processed*

2.2 Three-Dimensional Scanning of Patient's Residual Leg

The socket, pylon, foot and adapters were designed in computer aided design (CAD) software for finite element analysis (FEA) simulation purpose. The socket was constructed utilizing Autodesk Meshmixer (Autodesk, Inc., USA,) software with the 3D scanned residual leg model as the reference for accurate size and structure. To begin with, the region of interest was marked on the residual leg model surface by referring to the bony prominences of the residual leg. Then, the marked region was thickened to 6 mm referring to the thickness of the subject's conventional socket. In SolidWorks (Dassault Systèmes, France), a circular base was created and positioned below the thickened entity and were merged together to form a complete socket. The base served as the site for pylon attachment. SolidWorks (Dassault Systèmes, France) software was used to construct the pylon, adapters and the foot. The pylon was a tube with thickness of 5 mm and outer diameter 35 mm. Other components that were designed in SolidWorks were three adapters with different design and function which the design and

structure were improvised from conventional adapters. One of the adapters was for the socket and pylon connection and another two adapters were built to connect the foot and the pylon. To reduce the number of body and the complexity of the simulation, all adapters were merged together with the pylon as one body. The end design of the assembled prosthetic leg was shown in Fig. 3.

2.3 Meshing

STL files of all 3D models were imported into 3-Matic (Materialise N.V., Belgium) after designing steps were done. The parts comprised of residual leg, socket, pylon, and foot. They were appropriately aligned before remeshing process was done as seen in the Fig. 4. All components were then meshed with maximum element edge length of 5 mm. Then, the parts were solidified with mesh size of 5 mm using standard linear tetrahedral element. The total number of elements and nodes produced from remeshing process for the residual leg, socket, pylon, and foot were tabulated in Table 1.

Table 1 *List of parts, elements, and nodes of meshing*

Parts	Elements	Nodes
Stump	605010	8886
Socket	194723	14731
Pylon	62002	4326
Foot	408616	7954

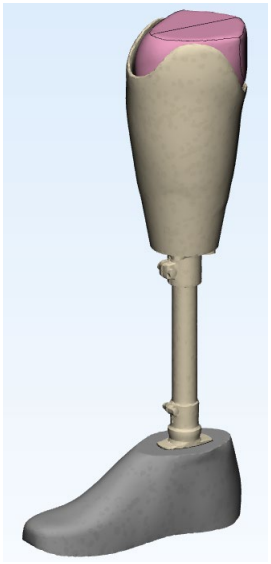

Fig. 3 *End design of prosthetic leg*

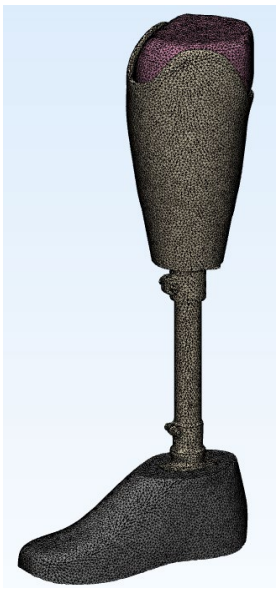

Fig. 4 *Meshed model of prosthetic leg*

2.4 Analysis Between Different Gait

The loading experienced by the prosthetic leg was simulated during phases in gait cycle which included the heel strike, midstance, and toe off [11]. The magnitude of load and the fixed region were different for each of the gait phases. The load for midstance was equivalent to half times the body weight of the subject which was 350 N. Whereas, the load applied during heel strike is correspond to 2.25 times the body weight which was 1575 N [12]. For toe off, the load applied was 3.5 times the body weight which was 2450 N [12]. The load applied for each of the phases was directed normal to the proximal surface of the clipped residual leg. The loading condition was adapted from prosthetic leg structural testing protocol complied with ISO 10328 [13]. The fixed regions for each gait phase in all axis were shown in Fig. 5 depending on the foot placement in contact with ground during gait cycle [14]. The materials assigned for each part were tabulated in Table 2 together with the Young's modulus and Poisson's ratio. For simplification purpose, all the finite element models were assumed to be isotropic, linearly elastic and homogenous [13]. The contact interactions set between all the finite element models were glued. All the models were set as deformable bodies to mimic real life circumstances. In addition, the selected method in controlling the contact was segment to segment because this method suitable to be used for fixed joint or contact [15].

Int. Journal of Integrated Engineering Vol. 16 No. 5 (2024) p. 214-223

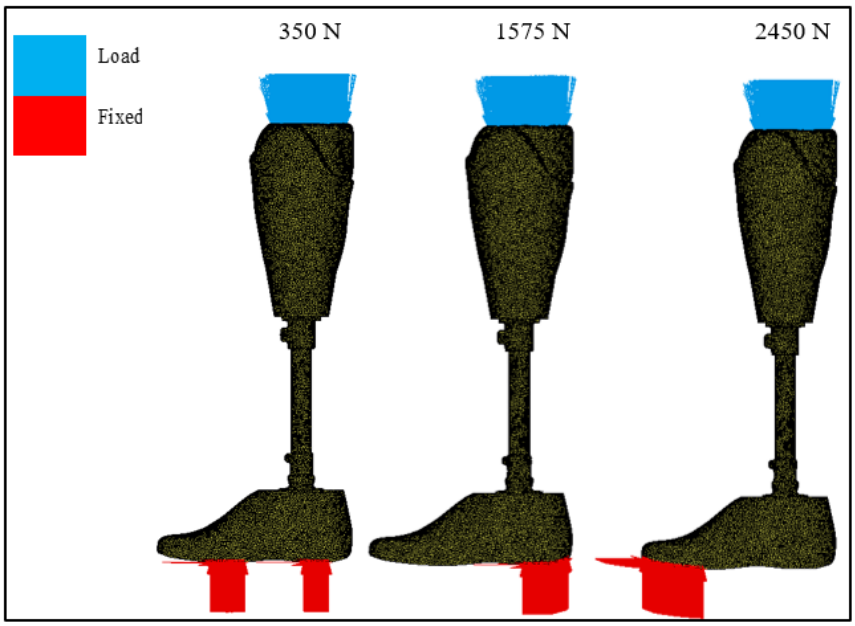

Fig. 5 *Placement of load and fixed region*

Table 2 *List of parts, materials, Young's modulus and the Poisson's ratio*

Parts	Materials	Young's modulus (MPa)	Poisson's ratio
Residual leg	Skin	20 [17]	0.48 [18]
Socket	ABS	2000 [19]	0.30 [19]
Pylon	ABS	2000 [19]	0.30 [19]
Foot	Polyurethane	1600 [20]	0.40 [20]

3. Results and Discussion

The results of von Mises Stress and the displacement of model with three different gait phases were discussed.

3.1 Von Mises Stress

The results von Mises Stress of the parts enabled to estimate the potential of yielding in all gait phases were discussed. The results obtained were illustrated in form of contour plot as shown in Fig. 6 and magnitudes were tabulated in Table 3. The results of each part were analysed for each of the sub-phase. During midstance, the peak stress at residual leg (0.24 MPa) was concentrated at the distal area of the residual leg. The peak stress of ABS socket was located at the base with 3.23 MPa magnitude. The ABS pylon experienced peak stress (4.89 MPa) at the posterior part of the foot adapter. Whereas, the part of the foot that experienced the highest stress was at the top surface in contact with foot adapter with 2.70 MPa. During heel strike, the maximum stress was observed to be situated at posterior compartment of the residual leg. The peak stress of the ABS socket (3.24 MPa) concentrated at the base. At the ABS pylon, the peak stress (13.41 MPa) was visible on the posterior shaft of the pylon. The foot experienced the peak stress at the top. During toe off, the peak stress of the residual leg (0.84 MPa) located at the posterior compartment. The peak stress of the socket (3.81 MPa) was concentrated at the base. The ABS pylon experienced the peak stress (20.86 MPa) at posterior pylon shaft. Whereas, the foot peak stress (18.77 MPa) was located at the lateral of the sole.

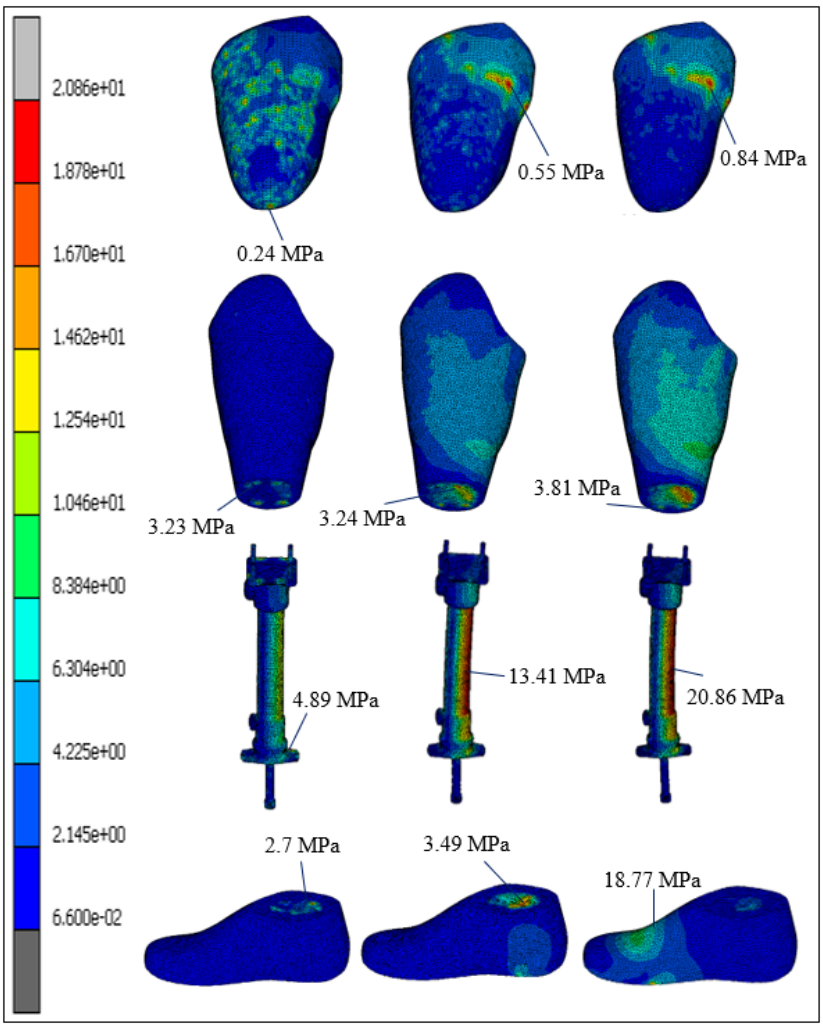

Fig. 6 *Von Mises stress distribution for residuum (first row), socket (second row), pylon (third row) and foot (forth row) for midstance (left), heel strike (middle) and toe off (right) gait phase*

In Table 3 the von Mises stress of each part were compared with yield stress of respective materials. For socket, pylon and foot, none of the maximum stress of these parts exceeding the yield stress of respective materials.

Table 3 *List of parts, gait phases, materials, maximum stress, and the yield*

Part	Gait Phase	Material	Maximum Stress (MPa)	Yield Stress (MPa)
Leg	Midstance	Skin	0.24	-
	Heel strike	Skin	0.55	-
	Toe off	Skin	0.84	-
Socket	Midstance	ABS	3.23	32 [20]
	Heel strike	ABS	3.24	32 [20]
	Toe off	ABS	3.81	32 [20]
Pylon	Midstance	ABS	4.89	32 [20]
	Heel strike	ABS	13.41	32 [20]
	Toe off	ABS	20.86	32 [20]
Foot	Midstance	PU	2.70	25 [21]
	Heel strike	PU	3.49	25 [21]
	Toe off	PU	18.77	25 [21]

Int. Journal of Integrated Engineering Vol. 16 No. 5 (2024) p. 214-223

3.2 Displacement

The displacement analysis during gait shown in Fig. 7 was very crucial because the stability of user can be estimated. From the contour plot, the deformation can be seen clearly during heel strike (54.95 mm). The load transfer from body weight to the prosthetic leg cause slight bending towards back. Whereas, during toe off phase the maximum displacement was 30.55 mm and the direction of the bending is towards back. During midstance phase, the prosthetic leg seems to have very low displacement (6 mm).

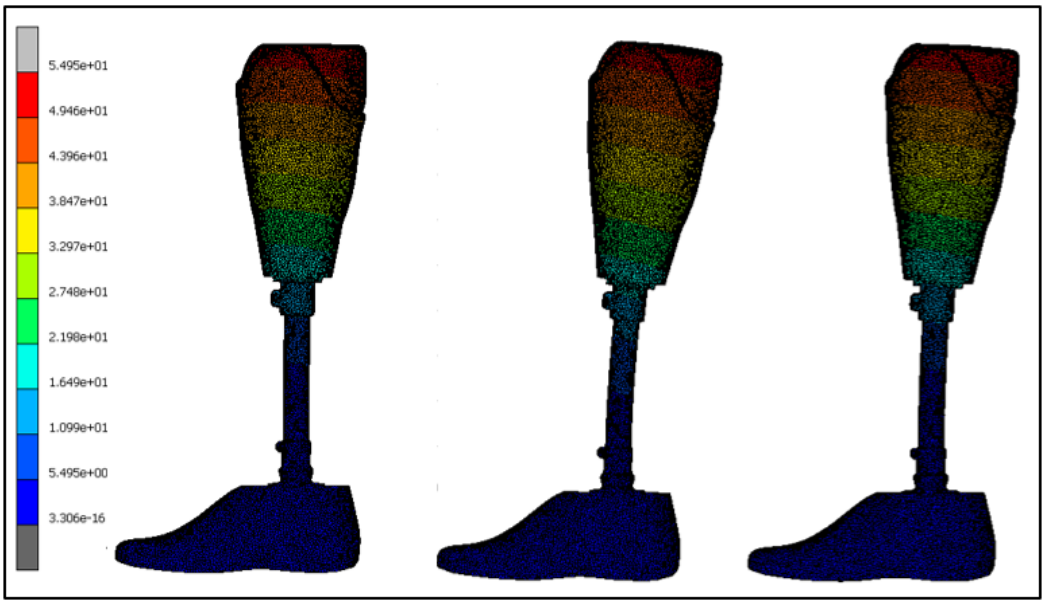

Fig. 7 *Displacement contour plot for midstance (left), toe off (middle) and heel strike (right)*

3.3 Discussion

Material selection is one of the crucial considerations for developing prosthetic components. The conventional socket usually made from polypropylene due to its lightweight properties [22]. Despite the advantage, the process of conventional socket fabrication was tedious, laborious and time consuming [23]. Besides, steel was replaced by aluminium and titanium as the material for conventional pylon [22]. However, the cost of the pylon made by these metals were considered high to low-income amputees. The overall cost of prosthetic leg can be reduced by implementing lower cost materials for fabricating the components. For instance, International Committee of the Red Cross (ICRC) introduced the usage of polypropylene material for developing the socket, pylon, adapters, and the cosmetic that offers acceptable quality and acknowledged by International Society for Prosthetics and Orthotics (ISPO) [24]. In this study, ABS material was implemented for the prosthetic socket and pylon to evaluate the potential of this material to replace existing material. In another study done by authors, prosthetic socket and pylon assigned with ABS material outperformed PLA material in mid stance phase hence it was selected for this study.

For von Mises stress analysis, during midstance phase, the residual leg experienced maximum stress that not surpassed the ultimate tensile stress (27.2 MPa) of the skin [25]. The maximum stress concentrated at the distal, pressure intolerant region of the residual leg that incapable of enduring high stress [26]. The socket and pylon assigned with ABS material were predicted to be able to sustain with the load applied as the result showed that the maximum stress of both parts not exceeded the yield strength of ABS material (32 MPa) [27]. Besides, the foot that was transferred with compressive, axial force from the pylon able to withstand the loading and not experiencing structural failure or yield. During heel strike, the posterior compartment of the residual leg experienced the maximum stress and was still able to tolerate with pressure from wall of the socket and no yielding was expected to occur. Meanwhile, the ABS socket able to sustain loading from residual leg. Besides, the axial loading from socket cause the posterior shaft of the pylon experienced high stress. However, the load was not adequate to yield the pylon as it was still in elastic deformation. Similarly, the foot was able to withstand the applied load without yield. Thus, the material and structure of the foot was durable enough to accommodate subject's load. During toe off, the maximum stress concentrated at the pressure tolerant area, the posterior compartment of residual leg. The ultimate tensile strength of skin was not exceeded thus no irreversible damage was expected. The ABS socket not experienced stress that can cause permanent damage or deformation. Likewise, the ABS pylon also has low possibility to deform permanently because the experienced maximum stress below the yield strength (32 MPa). Eventually, the foot maximum stress was quite high compared to other

phases. However, the loading was not adequate to destruct the foot and still able to return to original form once the load was removed.

The stability of the user during gait can be estimated by analysing the displacement of overall prosthetic leg. The alignment of prosthetic leg parts can affect the loading distribution hence the displacement also will be affected. From the contour plot, during toe off phase the maximum displacement was quite high. The loading causes the prosthetic leg pylon bends backwards. The bending can increase the pressure exerted to the back of the residual leg as shown in von Mises stress result. Nevertheless, the high pressure accumulated at pressure tolerance area which expected to not or gave little discomfort towards user. In addition, the stability of the user might be interrupted during toe off. During heel strike, there is slight bending of prosthetic leg. However, the bending is not very critical and acceptable because the flexibility enables natural body movement [28]. Since the maximum stress is still under allowable limit or yield strength (32 MPa) of respective material, the prosthetic leg can return to original state after unloaded.

In comparison with previous study, Mubarak et al. performed a simulation to study the influenced of different material: PLA, ABS and PP to the strength and displacement of the socket. In contrast to our socket design, their socket was designed with holes to reduce overall prosthesis weight. Similar to our study, the finite elements model consists of residual leg, socket, pylon and foot. The loading and boundary condition that represent the loading during mid stance of gait cycle were set. From the result, the ABS socket experienced the lowest peak von mises stress followed by PLA socket and finally PP socket. Next, the maximum displacement of ABS socket (0.206 mm) was lower than PP socket (0.262) but higher PLA socket (0.197 mm) [29]. In another study related to usage of ABS material for prosthetic component, Wan Fadzil et al. performed a simulation to compare the performance of different material of socket. Two common 3D printing material: PLA and ABS were compared. The base of the socket was fixed in all axis and entire inner wall of the socket was applied with load (600 N). According to the result, it was observed that maximum stress of ABS sockets lower than PLA socket, plus it did not exceed the yield strength of ABS material thus not yielding was expected [30].

The results obtained are acceptable for understanding the loading response in different gait phase and how the prosthetic leg components made from ABS behave. However, the study had several limitations that affect the reliability of load distribution throughout whole finite element models. The first limitation is the residual leg model which only consist of skin. The 3D model of the residual leg was obtained from 3D scanner which only provide the structure of external stump. The skin, soft tissue, and fat were assumed as one solid body similar to previous study [33]. Besides, tibia, femur tibia, patella and cartilage were excluded because there was no imaging data were acquired for the volunteer. Exclusion of the bone structures affect the loading distribution as the load was applied directly to the residual leg. In contrast to the previous studies, the load was applied to the bone [32-35]. In addition, the model of the stump was constructed using single volunteer's stump; thus, our study only limited to one morphology of stump [36]. Previous study proved that different morphology of stump affected the socket-residuum interaction [37]. For future study, population-representative can be instigated by implementing statistical shape model (SSM) [37]. Moreover, the residual limb was assumed to be assigned with linear material [38]. Nevertheless, it is acceptable as previous study found that there was no significant difference between hyper-elastic and linear model in pressure distribution plus computational time for linear model is shorter with linear model [38]. Lastly, there was no experimental validation done for the finite element models [39]. In previous study, Balaramakrishnan et al. conduct a study to validate the finite element model for role-over shape prosthetic foot evaluation with experimental analysis [40]. They fabricated a customized jig to position the prosthetic foot respected to simulation [40]. Due to time and budget limitations, we were forced to ruled out the experimental validation [40]. However, we did compare our study to previous study to verify the results.

4. Conclusion

From the overall finite element results, ABS have potential in development of physical prosthetic leg components as the initiative to lower the cost and provide better comfort to the user during gait. The results showed that socket and pylon made from ABS can withstand the load applied from the subject in different stance phase in gait cycle. The stress magnitude showed no possibility of yield for both parts. However, from the displacement result, the bending was quite high during heel strike that can cause imbalance to the user. To increase the stiffness of the three-dimensional printed parts the infill percentage should be increased accordingly, hence can reduced the bending. The precision of the results was acceptable but overall study still possessed some of limitations that can reduce the accuracy of the results. The 3D model of the stump is one of the limitations. The residual leg model only consists of skin and did not include all hard and soft tissues such as muscle and bone. Thus, the loading towards prosthetic leg did not mimic the loading of natural leg. Besides, the Young's modulus and Poisson's ratio for ABS was general and not specified for particular 3D printing setting. For future research, different infill percentage should be compared to verify the appropriate and acceptable value.

Acknowledgement

This research was financially funded by Universiti Teknologi Malaysia (UTM), under Prototype Development Fund 2 (PDF2) from Innovation and Commercialisation Centre (ICC) (grant no.: Q.J130000.4423.4J647) and by Universitas Sriwijaya Indonesia (UNSRI) (grant no.: Q.J130000.7323.1U051).

Conflict of Interest

Authors declare that there is no conflict of interests regarding the publication of the paper.

Author Contribution

The authors confirm contribution to the paper as follows: ***study conception and design:*** *M.H.B., M.H.R.;* ***data collection:*** *M.H.B., M.H.R.;* ***analysis and interpretation of results:*** *M.H.B., A.M.A.R., N.N.A.A.A.;* ***draft manuscript preparation:*** *M.H.B., A.M.A.R., N.N.A.A.A., M.H.R.;* ***final manuscript preparation:*** *M.H.B., M.H.R. All authors reviewed the results and approved the final version of the manuscript.*

References

[1] Karim, H. H. A., & Ming, C. P. (2020). Characteristics and prosthesis usage of amputees attending medical rehabilitation services in Malaysia. *Medical Journal of Malaysia, 75,* 519–524.
[2] Jia, X., Zhang, M., & Lee, W. C. C. (2004). Load transfer mechanics between trans-tibial prosthetic socket and residual limb - Dynamic effects. *Journal of Biomechanics, 37,* 1371–1377.
[3] Omasta, M., Paloušek, D., Návrat, T., & Rosický, J. (2012). Finite element analysis for the evaluation of the structural behaviour, of a prosthesis for trans-tibial amputees. *Medical Engineering and Physics, 34,* 38–45.
[4] Eshraghi, A., Abu Osman, N. A., Karimi, M., Gholizadeh, H., Soodmand, E., & Wan Abas, W. A. B. (2014). Gait biomechanics of individuals with transtibial amputation: Effect of suspension system. PLoS ONE, 9, 1–12.
[5] Esquenazi, A. (2014). Gait analysis in lower-limb amputation and prosthetic rehabilitation. *Physical Medicine and Rehabilitation Clinics of North America, 25,* 153–167.
[6] Ali, I., Kumar, R., & Singh, Y. (2014). Finite element modelling and analysis of trans-tibial prosthetic socket. *Global Journal of Researches in Engineering, 14,* 42–50.
[7] Dickinson, A. S., Steer, J. W., & Worsley, P. R. (2017). Finite element analysis of the amputated lower limb: A systematic review and recommendations. *Medical Engineering and Physics, 43,* 1–18.
[8] Rohjoni, F. M., Patar, M. N. A. A., Mahmud, J., Lee, H., & Hanafusa, A. (2020). Finite element analysis of a transtibial prosthetic during gait cycle International. *Journal of Mechanical Engineering and Robotics Research, 9,* 764–770.
[9] Rochlitz, B., & Pammer, D. (2017). Design and analysis of 3D printable foot prosthesis. *Periodica Polytechnica Mechanical Engineering, 61,* 282–287.
[10] Ahmad Fozi, M. A., Salleh, M. N., & Ismail, K. A. (2019). Development of 3D-printed customized facial padding for burn patients. *Rapid Prototyping Journal, 25,* 55–61.
[11] Di Gregorio, R., & Vocenas, L. (2021). Identification of gait-cycle phases for prosthesis control. *Biomimetics, 6(2).*
[12] Guo, Y., Zhang, X., & Chen, W. (2009). Three-dimensional finite element simulation of total knee joint in gait cycle. *Acta Mechanica Solida Sinica, 22(4),* 347–351.
[13] Baharuddin, M. H., Rashid, A. M. A., Nasution, A. K., Seng, G. H., & Ramlee, M. H. (2021). Patient-specific design of passive prosthetic leg for transtibial amputee: Analysis between two different designs. *Malaysian Journal of Medicine and Health Sciences, 17(4),* 228–234.
[14] Kahtan, Y. Y. (2019). Below knee prosthesis modal analysis. *International Journal of Mechanical Engineering and Technology, 10(1),* 2127–2132.
[15] Mayer, M. H., & Gaul, L. (2007). Segment-to-segment contact elements for modelling joint interfaces in finite element analysis. *Mechanical Systems and Signal Processing, 21(2),* 724–734.
[16] Pawlaczyk, M., Lelonkiewicz, M., & Wieczorowski, M. (2013). Age-dependent biomechanical properties of the skin. *Postepy Dermatologii i Alergologii, 30(5),* 302–306.
[17] Li, C., Guan, G., Reif, R., Huang, Z., & Wang, R. K. (2012). Determining elastic properties of skin by measuring surface waves from an impulse mechanical stimulus using phase-sensitive optical coherence tomography. *Journal of the Royal Society Interface, 9(70),* 831–841.
[18] En-Naji, A., Mouhib, N., Lahlou, M., Farid, H., & El Ghorba, M. (2019). Change of experimental young's modulus with increasing temperature for an ABS material subjected to tensile test. *ARPN Journal of Engineering and Applied Sciences, 14(3),* 708–717.
[19] Linul, E., & Marsavina, L. (2011). Prediction of fracture toughness for open cell polyurethane foams by finite-element micromechanical analysis. *Iranian Polymer Journal, 20(9),* 735-746.

[20] Singh, S., Prakash, C., Ramakrishna, S., & Krolczyk, G. (2020). Advances in Materials Processing. In Key Engineering Materials. pp. 1-778.
[21] M. F. Ashby. (2011). *Data for engineering materials*. In Materials Selection in Mechanical Design (4th ed.). Elsevier, pp. 495-523.
[22] Che Me, R., Ibrahim, R., & Md. Tahir, P. (2012). Natural based biocomposite material for prosthetic socket fabrication. *International Journal on Sustainable Tropical Design Research & Practice, 5(1),* 27–34.
[23] Cabrera, I. A., Pike, T. C., McKittrick, J. M., Meyers, M. A., Rao, R. R., & Lin, A. Y. (2021). Digital healthcare technologies: Modern tools to transform prosthetic care. *Expert Review of Medical Devices, 18,* 129–144.
[24] Ratto, M., Hiansen, J.Q., Marshall, J., Kaweesa, M., Taremwa, J., Heang, T., Kheng, S., Teap, O., Mchihiyo, D., Onesmo, R., & Moshi, B. (2021). An international, multicenter field trial comparison between 3d-printed and icrc-manufactured transtibial prosthetic devices in low-income countries. *Journal of Prosthetics and Orthotics, 33(1),* 54–69.
[25] Gallagher A.J., Ní Anniadh A., Bruyere K., Otténio M., Xie H., & Gilchrist M.D. (2012). Dynamic tensile properties of human skin. IRCOBI Conf. Proc. Dublin, 494–502.
[26] Powelson, T., & Yang, J. (2011). Prosthetics for transtibial amputees - A literature survey. Proceedings of the ASME Design Engineering Technical Conference, 3(PARTS A AND B), 753-764.
[27] A. Bhaduri. (2018). Tension. In Mechanical Properties and Working of Metals and Alloys. Springer, pp. 3-93.
[28] Saad, H., Abdullah, M. Q., & Wasmi, H. R. (2017). The modeling and effect of FEM on prosthetic limb. *International Journal of Cell Science and Biotechnology, 7(3),* 892–895.
[29] Mubarak, A. J. M., Rashid, A. M. A., Wahab, A. A., Seng, G. H., & Ramlee, M. H. (2021). Customized Designs and Biomechanical Analysis of Transtibial Prosthetic Leg. Journal of Physics: Conference Series, 1-8.
[30] Fatimatul, W., Wan, A., Mazlan, M. A., & Hanapiah, F. A. (2019). 3D Printed Lower-Limb Socket for Prosthetic Legs. *International Journal Of Engineering Research And Management, 6(3),* 14–18.
[31] Steer, J. W., Worsley, P. R., Browne, M., & Dickinson, A. (2020a). Key considerations for finite element modelling of the residuum–prosthetic socket interface. *Prosthetics and Orthotics International. 45(2),* 138-146.
[32] Portnoy, S., Siev-Ner, I., Yizhar, Z., Kristal, A., Shabshin, N., & Gefen, A. (2009). Surgical and morphological factors that affect internal mechanical loads in soft tissues of the transtibial residuum. *Annals of Biomedical Engineering, 37(12),* 2583–2605.
[33] Portnoy, S., Yizhar, Z., Shabshin, N., Itzchak, Y., Kristal, A., Dotan-Marom, Y., Siev-Ner, I., & Gefen, A. (2008). Internal mechanical conditions in the soft tissues of a residual limb of a trans-tibial amputee. *Journal of Biomechanics, 41(9),* 1897–1909.
[34] Portnoy, S., Siev-Ner, I., Shabshin, N., Kristal, A., Yizhar, Z., & Gefen, A. (2009). Patient-specific analyses of deep tissue loads post transtibial amputation in residual limbs of multiple prosthetic users. *Journal of Biomechanics, 42(16),* 2686–2693.
[35] Portnoy, S., Yarnitzky, G., Yizhar, Z., Kristal, A., Oppenheim, U., Siev-Ner, I., & Gefen, A. (2007). Real-time patient-specific finite element analysis of internal stresses in the soft tissues of a residual limb: A new tool for prosthetic fitting. *Annals of Biomedical Engineering, 35(1),* 120–135.
[36] Dakhil, N., Tarrade, T., Behr, M., Mo, F., Evin, M., Thefenne, L., Liu, T., & Llari, M. (2020). Influence of the scale reduction in designing sockets for trans-tibial amputees. Proceedings of the Institution of Mechanical Engineers, Part H: Journal of Engineering in Medicine, 234(8), 761–768.
[37] Steer, J. W., Worsley, P. R., Browne, M., & Dickinson, A. S. (2020b). Predictive prosthetic socket design: part 1—population-based evaluation of transtibial prosthetic sockets by FEA-driven surrogate modelling. *Biomechanics and Modeling in Mechanobiology, 19(4),* 1331–1346.
[38] Ballit, A., Mougharbel, I., Ghaziri, H., & Dao, T. T. (2020). Fast soft tissue deformation and stump-socket interaction toward a computer-aided design system for lower limb prostheses*. Innovation and Research in Biomedical Engineering, 41(5),* 276–285.
[39] Steer, J. W., Grudniewski, P. A., Browne, M., Worsley, P. R., Sobey, A. J., & Dickinson, A. S. (2020). Predictive prosthetic socket design: part 2—generating person-specific candidate designs using multi-objective genetic algorithms. *Biomechanics and Modeling in Mechanobiology, 19(4),* 1347–1360.
[40] Balaramakrishnan, T. M., Natarajan, S., & Srinivasan, S. (2020). Roll-over shape of a prosthetic foot: A finite element evaluation and experimental validation. *Medical and Biological Engineering and Computing, 58(10),* 2259–2270.